

Report

Modelling and simulation of $\text{TNF}\alpha$ secretion in macrophages



University of Heidelberg, Germany

Institute of Pharmacy and Molecular Biotechnology

IPMB

Stefan Quint

Matrikel No. 2234208

Heidelberg, 26th of June 2005

Contents

1	Introduction	2
2	Model	4
2.1	Cytoplasmic $I\kappa k$	4
2.2	Cytoplasmic $NF\kappa B/I\kappa B$	4
2.3	Cytoplasmic $NF\kappa B$	6
2.4	Cytoplasmic $I\kappa B$	7
2.5	Nuclear $NF\kappa B$	7
2.6	$I\kappa B$ -mRNA	8
2.7	$TNF\alpha$ -mRNA	8
2.8	Cellular $TNF\alpha$	9
2.9	Soluble $TNF\alpha$	9
2.10	Nuclear $I\kappa B$	10
2.11	Nuclear $NF\kappa B/I\kappa B$	10
3	Hypothetical inhibitor	10
3.1	Inhibitor-mRNA	11
3.2	Cytoplasmic inhibitor	11
3.3	Nuclear inhibitor	11
4	Simulation results	13
4.1	Initial conditions and a steady state	13
4.2	Comparison of model prediction and measured $TNF\alpha$	13
4.3	Time courses of all fourteen states	15
5	Conclusions and outlook	24
6	Appendix	26
6.1	MADONNA	26
6.2	Modelling a time delay	28
6.3	MUSCOD	30
6.3.1	c-File	30
6.3.2	Dat-File	35

Abstract

The LPS induced signalling pathway, which leads to secretion of $\text{TNF}\alpha$ is modelled using fourteen ordinary differential equations. Here, the complex system is reduced to its major components in order to create a comprehensible model. The model describes the qualitative behaviour of $\text{TNF}\alpha$ -secretion with satisfactory accuracy. This may indicate that the knowledge we use to model the LPS induced signalling already includes the critical steps in this process. Even if the model still has some major limitations in describing $\text{TNF}\alpha$ -secretion, it already helps to improve the notion of the complex regulation in LPS signalling, which makes it a valuable support in the experimental work.

1 Introduction

Macrophages are part of the innate immunity - the "first line defence". These phagocytotic cells are the first, which get in touch with invading pathogens. To recognize the pathogens, macrophages carry different receptors on their surface. One of them is toll-like receptor 4 (TLR4). This receptor signalizes indirectly the existence of lipopolysaccarides (LPS), which are major components of the outer membrane of Gram-negative bacteria [1]. The first step, which leads to the signal transduction by TLR4 involves the LPS binding protein (LBP). LBP is an acute phase protein produced by the liver. It circulates in the bloodstream and recognizes LPS. LBP binds to LPS forming a complex which associates with mCD14, a membrane bound protein on the macrophage's surface. CD14 enables LPS to be transferred to the LPS receptor complex, which is composed of TLR4 and MD-2 [2]. As soon as TLR4 is associated with LPS, the receptor induces a signalling cascade into the nucleus, which leads to the activation of $\text{NF}\kappa\text{B}$ regulated genes. This signalling involves the cytoplasmic domain of TLR4, which is called TIR domain. In the early signalling, the association of LPS with TLR4 on the extracellular side causes the TIR domain to bind and activate the adaptor protein MyD88. This protein has a death domain at its N-terminal end, which mediates the interaction with the death domain of a further protein, called IRAK. IRAK, a serine/threonine kinase, then induces a cascade of kinase activation which subsequently activates TRAF6. This kinase again activates two other kinases namely $\text{I}\kappa\text{k}\alpha$ and $\text{I}\kappa\text{k}\beta$, which associate to form a dimer called $\text{I}\kappa\text{k}$.

I κ k phosphorylates I κ B, an inhibitor tightly bound to NF κ B. Phosphorylation of I κ B leads to its dissociation from NF κ B and its degradation by proteasoms. This enables NF κ B to translocate into the nucleus where it upregulates transcription of I κ B and a large number of other genes including TNF α . Newly synthesized TNF α is firstly anchored to the membrane. Secretion of TNF α takes place when TACE, a membrane bound enzyme, cleaves the protein from its anchoring transmembrane domain. I κ B serves as a negative feedback regulator. It can enter the nucleus, remove NF κ B from DNA, and export the complex back to the cytoplasm to restore the original latent state [3]. The whole signalling pathway is more complex as it can be described here. A more detailed description of the events during the TLR4 signalling is given in [2] and [4].

In this work, we concentrated on the expression of TNF α (Tumor Necrosis Factor), which is one of the NF κ B activated genes. TNF α is a cytokine, which stimulates inflammatory reactions by activating macrophages, neutrophils and endothelial cells. In severe infections, TNF α is produced in large amounts and has systemic effects, including fever and cachexia. Very large amounts of TNF α can cause intravascular thrombosis and shock, which is usually lethal. The lack of effective therapeutic approaches for septic shock gives rise to the death of many people world-wide. Therefore, research denotes to the molecular basis of LPS signal transduction is an area of great interest. The true nature of LPS signalling and how it might be controlled and regulated is still poorly understood. The aim of this project was to establish a mathematical model of LPS induced TNF α -production, which improves the understanding of the system regulation. Here the role of an unknown inhibitor, which is involved in the regulation of the TNF α production was of great interest. A number of proteins, which inactivate TLR4 signalling have been identified and described [2]. All of them block the signalling pathway on an early stage, which directly influence the amount of free NF κ B. ST2 and SIGIRR, for instance, are cell-surface receptors with TIR domains, which inhibit TLR4 by sequestering signalling proteins from the pathway. Traid3 has been identified as an ubiquitin ligase that ubiquitylates TLR4, leading to its down-regulation and degradation. However the experimental results of Dr. Alexei Gratchev imply that there must be a negative regulation on a later stage, which has no influence on the NF κ B concentration in the cell.

2 Model

The signal transduction, which leads to the secretion of $\text{TNF}\alpha$ is a highly complex process. To model the system, we reduce it to its main components. This enables us to get a clear and comprehensible model, which still describes the behaviour of the complex system. The simplified signalling pathway, which was assumed for the modelling is shown in Fig. 1. The pathway is modelled by fifteen ODEs (ordinary differential equations), which are explained in the following.

All states and parameters, which will be described in this section are summarized in Tab. 1 and Tab. 2.

2.1 Cytoplasmic $\text{I}\kappa\text{k}$

Referring to the experimental conditions, the amount of LPS and LBP in the media is considered to be much higher than the amount of LPS receptors. In this case, the association kinetics of mCD14 with LPS/LBP-complex can be neglected and we may assume that every LPS receptor complex is loaded with LPS most of the time. Therefore, the amount of activated TLR4 is assumed to be constant. In this model all steps beginning with MyD88 recruitment up to $\text{I}\kappa\text{k}$ activation are united into one single step. Moreover $\text{I}\kappa\text{k}$ complex is considered as a single protein. The dynamics that lead to its formation have been disregarded. We assumed that the amount of activated $\text{I}\kappa\text{k}$ increases linearly with the number of activated TLR4 receptors. We denote the concentration of $\text{I}\kappa\text{k}$ by x_1 and formulate the first equation,

$$\frac{dx_1}{dt} = k_{\text{act}} - k_{\text{inact}}x_1 \quad (1)$$

k_{act} is a constant activation of $\text{I}\kappa\text{k}$ due to TLR4 activation. The term $k_{\text{inact}}x_1$ describes the inactivation of $\text{I}\kappa\text{k}$, which should be proportional to the concentration of activated $\text{I}\kappa\text{k}$.

2.2 Cytoplasmic $\text{NF}\kappa\text{B}/\text{I}\kappa\text{B}$

The phosphorylation of $\text{NF}\kappa\text{B}/\text{I}\kappa\text{B}$ complex in the cytoplasm by $\text{I}\kappa\text{k}$, leads to the degradation of $\text{I}\kappa\text{B}$ and the release of free $\text{NF}\kappa\text{B}$. The phosphorylation should be proportional to the concentration of activated $\text{I}\kappa\text{k}$. If we assume simple enzyme

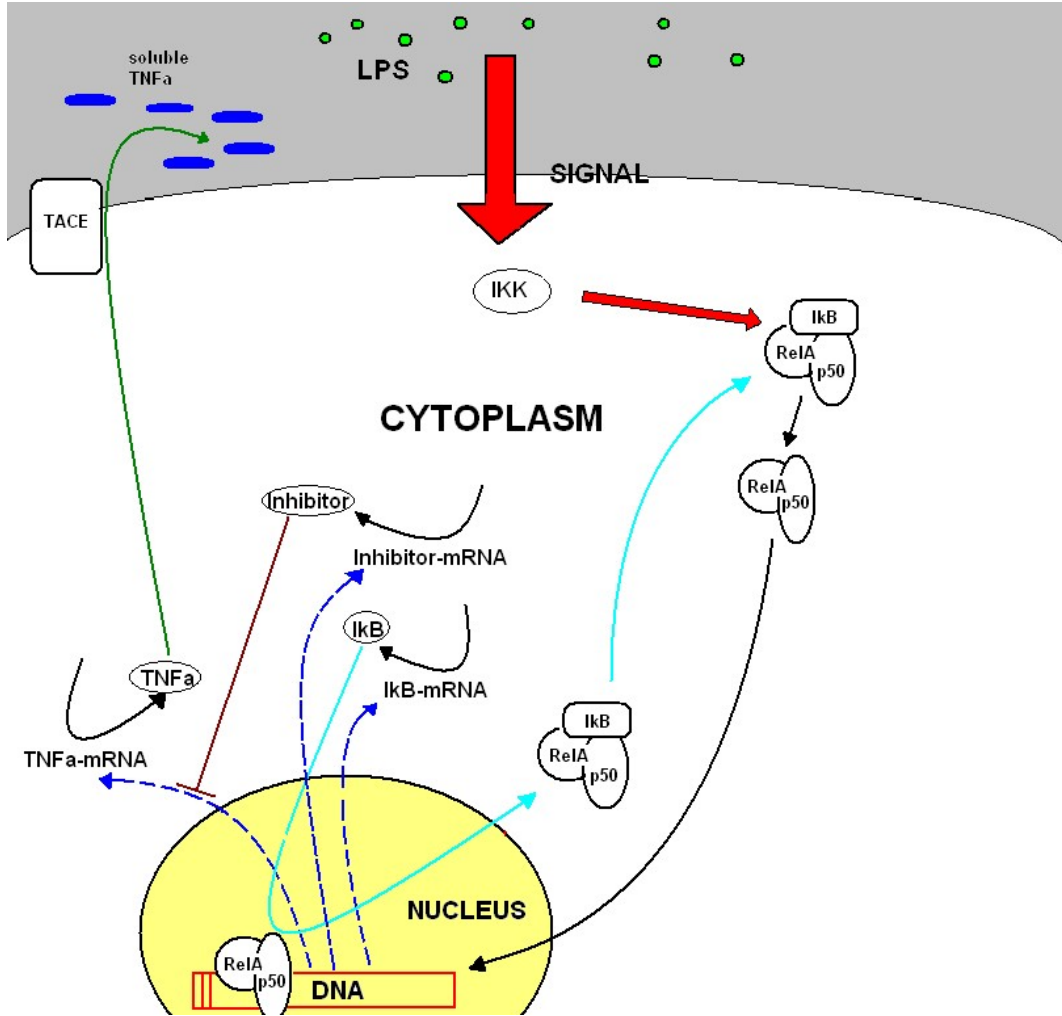


Figure 1: The scheme summarizes the events described in the model. LPS in the extracellular space (green coloured) induces the activation of $I\kappa k$. Activated $I\kappa k$ phosphorylates $NF\kappa B/I\kappa B$ complex, which leads to the degradation of $I\kappa B$ and release of $NF\kappa B$. $NF\kappa B$ enters the nucleus (yellow), binds to its response elements and activates the synthesis of $TNF\alpha$, $I\kappa B$ and inhibitor mRNA (blue dashed arrows). These transcripts are then translated into the corresponding proteins (black arrows). Cellular $TNF\alpha$ is released through the activity of membrane bound TACE. $TNF\alpha$ secretion is lowered when the cytoplasmic inhibitor enters the nucleus and inhibits synthesis of $TNF\alpha$ -mRNA. Note that the existence of this inhibitor is purely hypothetically and so far was not proved experimentally.

kinetics for the phosphorylation reaction, the change in NF κ B/I κ B concentration is given by the following equation,

$$\frac{dx_2}{dt} = -x_1 v_{IKK} \frac{x_2}{K_{IKK} + x_2} - k_{\text{deg}}^{\text{NI}} x_2 \quad (2)$$

Here, x_2 is the concentration of NF κ B/I κ B in the cytoplasm. K_{IKK} is the Michaelis-Menten constant of I κ k and v_{IKK} is its maximum conversion-rate. Following Hoffmann et al. [5], we consider a spontaneous degradation of complex bound I κ B, which is proportional to the NF κ B/I κ B concentration. This is described in the second term where $k_{\text{deg}}^{\text{NI}}$ is the degradation rate of complex bound I κ B. For the complete mass balance of cytoplasmic NF κ B/I κ B, we have to consider two more contributions. The concentration of the complex will increase when free cytoplasmic I κ B and NF κ B associate, which we consider as a bimolecular reaction. Moreover, newly-synthesized I κ B can enter the nucleus, remove NF κ B from DNA, and export the complex back to the cytoplasm. Taking these contributions into consideration we extend (2) and obtain,

$$\frac{dx_2}{dt} = -x_1 v_{IKK} \frac{x_2}{K_{IKK} + x_2} + k_{\text{ass}}^{\text{NI}} x_3 x_4 + k_{\text{ex}}^{\text{NI}} x_{11} - k_{\text{deg}}^{\text{NI}} x_2 \quad (3)$$

where x_3 is the concentration of free cytoplasmic NF κ B, x_4 is the concentration of free cytoplasmic I κ B and $k_{\text{ass}}^{\text{NI}}$ is the association rate of the two proteins. x_{11} is the concentration of NF κ B/I κ B complex in the nucleus and $k_{\text{ex}}^{\text{NI}}$ is its export rate into the cytoplasm. A dissociation of NF κ B/I κ B complex is neglected within our model. This can be justified by the fact that the complex is very stable. Experimental results of Hoffmann et al. [5] showed that the dissociation rate is only about one thousandth of the association rate.

2.3 Cytoplasmic NF κ B

The dynamics of cytoplasmic NF κ B is described by equation (4). The first term describes the release of NF κ B due to the phosphorylation of NF κ B/I κ B by I κ k in the cytoplasm,

$$\frac{dx_3}{dt} = x_1 v_{IKK} \frac{x_2}{K_{IKK} + x_2} - k_{\text{ass}}^{\text{NI}} x_3 x_4 - k_{\text{up}}^{\text{N}} x_3 + k_{\text{ex}}^{\text{N}} x_5 + k_{\text{deg}}^{\text{NI}} x_2 \quad (4)$$

The second term describes a decrease of the concentration when free cytoplasmic I κ B and NF κ B associate to form NF κ B/I κ B complex. Free cytoplasmic NF κ B is then

taken up into the nucleus as described in the third term. We assume this uptake to be proportional to the concentration of NF κ B in the cytoplasm, with the rate k_{up}^{N} . Moreover, we assume that a small fraction of the nuclear NF κ B do not bind to DNA, because of the saturation of DNA binding sites for instance. Therefore, some NF κ B is exported again into the cytoplasm as described by the fourth term. By analogy with the NF κ B uptake we consider the export of nuclear NF κ B (denoted by x_5) to be proportional to its concentration, where k_{ex}^{N} is the export rate. The last term represents the increase in NF κ B concentration when cytoplasmic NF κ B/I κ B dissociates due to constitutive I κ B degradation.

2.4 Cytoplasmic I κ B

The change of the cytoplasmic I κ B concentration is modelled by,

$$\frac{dx_4}{dt} = -k_{\text{ass}}^{\text{NI}}x_3x_4 + k_{\text{prod}}^{\text{I}}x_6 - k_{\text{up}}^{\text{I}}x_4 + k_{\text{ex}}^{\text{I}}x_{10} - k_{\text{deg}}^{\text{I}}x_4 - x_1v_{\text{IKK}}\frac{x_4}{K_{\text{IKK}} + x_4} \quad (5)$$

The first term describes the association I κ B and NF κ B, which results in the decrease of I κ B concentration. I κ B concentration increases when I κ B-mRNA (denoted by x_6) is translated. This is considered by the second term. Here, $k_{\text{prod}}^{\text{I}}$ is the rate of mRNA translation. The third term represents uptake of cytoplasmic I κ B into the nucleus with uptake rate k_{up}^{I} . Export of nuclear I κ B (x_{10}) into the cytoplasm is considered by the fourth term. The next to the last term represents constitutive degradation of I κ B with degradation rate $k_{\text{deg}}^{\text{I}}$. We assumed also that free cytoplasmic I κ B is phosphorylated by I κ k and afterwards degraded. This is described by the last term.

2.5 Nuclear NF κ B

Nuclear concentration of NF κ B depends on the one hand on its transport into and out of the nucleus. This is considered by the first two terms of eq. (6), where k_{ex}^{N} is the export rate and k_{up}^{N} is the uptake rate. We consider the transport processes to be proportional to nuclear and cytoplasmic NF κ B concentration respectively. Concentration of free nuclear NF κ B decreases also if I κ B enters the nucleus and associates with NF κ B. This is considered by the last term of eq. (6). Here, $k_{\text{ass}}^{\text{nNI}}$ is the association rate of I κ B and NF κ B in the nucleus. We assume that this rate differs from

the association rate in the cytoplasm, because nuclear NF κ B is mainly DNA bound, which should affect I κ B NF κ B association.

$$\frac{dx_5}{dt} = k_{\text{up}}^{\text{N}}x_3 - k_{\text{ex}}^{\text{N}}x_5 - k_{\text{ass}}^{\text{nNI}}x_5x_{10} \quad (6)$$

2.6 I κ B-mRNA

Nuclear NF κ B binds to NF κ B response elements in order to activate the transcription of several genes, with I κ B among them. Following Lipniacki et al. [6] we consider the transcription of NF κ B regulated genes to be proportional to nuclear NF κ B concentration. Export of mRNA into the cytoplasm is also assumed to be proportional to its concentration in the nucleus. The concentration of I κ B-mRNA in the cytoplasm should, therefore, be proportional to the nuclear NF κ B concentration, the rate of mRNA synthesis and the rate of mRNA export. Instead of introducing two rate constants $k_{\text{prod}}^{\text{mI}}$ and $k_{\text{ex}}^{\text{mI}}$, we can unite them into a single rate constant, which we call $k_{\text{prex}}^{\text{mI}}$. Thus, increase in the concentration of cytoplasmic I κ B-mRNA is described by the first term of eq. (7). The second term in eq. (7) considers degradation of I κ B-mRNA, which should be proportional to its concentration and degradation rate $k_{\text{deg}}^{\text{mI}}$.

$$\frac{dx_6}{dt} = k_{\text{prex}}^{\text{mI}}x_5 - k_{\text{deg}}^{\text{mI}}x_6 \quad (7)$$

2.7 TNF α -mRNA

Beside the transcription of I κ B, NF κ B induces a synthesis of TNF α -mRNA. The assumptions made in eq. (8) are analogous to these in equation (7). Here, the factor $k_{\text{prex}}^{\text{mT}}$ in the first term represents both export of TNF α -mRNA and its synthesis. $k_{\text{deg}}^{\text{mT}}$ represents the degradation rate of TNF α -mRNA. The last term describes inhibition of TNF α -mRNA synthesis due to the presence of nuclear inhibitor. This influence is discussed more detailed in section 3.3.

$$\frac{dx_7}{dt} = k_{\text{prex}}^{\text{mT}}x_5 - k_{\text{deg}}^{\text{mT}}x_7 - k_{\text{inh}}x_{14} \quad (8)$$

2.8 Cellular TNF α

The concentration of cellular TNF α increases when TNF α -mRNA is translated. We consider this translation to be proportional to the amount of available mRNA in the cytoplasm. This contribution is represented by the first term of eq. (9). Here, the factor k_{prod}^T is the translation rate of TNF α -mRNA. Cellular TNF α is a membrane bound protein. The soluble form of TNF α is produced by TACE, which cleaves TNF α from its transmembrane domain. We assume that activity of TACE can be described by Monod kinetics. Therefore, the concentration of cellular TNF α should therefore decrease as described by the kinetics represented in the last term of equation (9). Here, K_{TACE} is the Michaelis-Menten constant of TACE and v_{TACE} is its maximum cleaving-rate. The constant k_{tace} is the amount of membrane bound TACE, which we assume to be constant.

$$\frac{dx_8}{dt} = k_{\text{prod}}^T x_7 - k_{\text{tace}} v_{TACE} \frac{x_8}{K_{TACE} + x_8} \quad (9)$$

2.9 Soluble TNF α

We propose the following equation for the dynamics of soluble TNF α ,

$$\frac{dx_9}{dt} = k_{\text{tace}} v_{TACE} \frac{x_8}{K_{TACE} + x_8} - k_T x_9 \quad (10)$$

The concentration of soluble TNF α increases when TACE cleaves membrane bound TNF α , as described by the first term. The last term considers binding of soluble TNF α by TNF α receptors in the media. These receptors are located on the surface of macrophages (note that around 800000 cells are present in the experimental media) or they may be secreted by macrophages. We assume that the TNF α receptor concentration is much higher than the concentration of soluble TNF α and consider the concentration of free TNF α receptors to be constant. The decrease in the soluble TNF α concentration is assumed to be proportional to soluble TNF α concentration, as described by the last term, where k_T is the association rate of TNF α and TNF α receptor. It is important to remark that x_9 actually represents the soluble TNF α concentration per cell volume. To calculate the real concentration in the media x_9 has to be multiplied with $\frac{V_{\text{cell}}}{V_{\text{media}}}$, the cell volume's fraction of the media volume.

$$\frac{dx_9}{dt} = k_{\text{tace}} v_{TACE} \frac{x_8}{K_{TACE} + x_8} - k_T x_9 \quad (11)$$

2.10 Nuclear I κ B

The assumptions made in equation (12) are analogous to these in equation (6). I κ B is taken up from the cytoplasm into the nucleus. This is considered by the first term, where k_{up}^{I} represents the uptake rate. Export of I κ B with the export rate k_{ex}^{I} is described by the second term. The last term represents association of I κ B and NF κ B with association rate $k_{\text{ass}}^{\text{nNI}}$.

$$\frac{dx_{10}}{dt} = k_{\text{up}}^{\text{I}}x_4 - k_{\text{ex}}^{\text{I}}x_{10} - k_{\text{ass}}^{\text{nNI}}x_5x_{10} \quad (12)$$

2.11 Nuclear NF κ B/I κ B

The concentration of nuclear NF κ B/I κ B increases when I κ B and NF κ B associate. This association is represented by the first term. The last term describes the export of nuclear NF κ B/I κ B into the cytoplasm. Due to the strong export signal of the complex, we assume that there is no uptake of NF κ B/I κ B into the nucleus.

$$\frac{dx_{11}}{dt} = k_{\text{ass}}^{\text{nNI}}x_5x_{10} - k_{\text{ex}}^{\text{nNI}}x_{11} \quad (13)$$

3 Hypothetical inhibitor

Experimental observations show that in spite of the constant LPS activation the concentration of TNF α -mRNA decreases (Dr. Alexei Gratchev, personal communication). Moreover, it is observed that free NF κ B concentration remains constant under these conditions. We conclude from the observations that there exists an inhibitor, which may act on the following ways:

- 1.) The inhibitor lowers gene expression of TNF α , for instance, by acting as transcription factor or co-inhibitor.
- 2.) The inhibitor lowers the stability of TNF α -mRNA.

Due to the lack of experimental data, it is difficult to determine, which scenario has more relevance. Therefore the following assumptions are only a hypothesis which has not yet been experimentally proved. We assume that the inhibitor affects gene expression of TNF α acting as a transcription factor for instance. To model this, we introduce three more equations which are explained in the following.

3.1 Inhibitor-mRNA

We assume that a synthesis of the hypothetical inhibitor-mRNA is regulated by NF κ B. Therefore, we assume that the rate of mRNA synthesis is proportional to the concentration of nuclear NF κ B, as it is described in eq. (14). In equivalence to equation (8) and equation (7), the factor $k_{\text{prex}}^{\text{mInh}}$ represents both export of mRNA and its synthesis. The degradation of inhibitor-mRNA with a degradation rate $k_{\text{deg}}^{\text{mInh}}$ is described by the last term.

$$\frac{dx_{12}}{dt} = k_{\text{prex}}^{\text{mInh}} x_5 - k_{\text{deg}}^{\text{mInh}} x_{12} \quad (14)$$

3.2 Cytoplasmic inhibitor

$$\frac{dx_{13}}{dt} = k_{\text{prod}}^{\text{Inh}} x_{12} - k_{\text{up}}^{\text{Inh}} x_{13} + k_{\text{ex}}^{\text{Inh}} x_{14} - k_{\text{deg}}^{\text{Inh}} x_{13} \quad (15)$$

The translation of inhibitor-mRNA is considered to be proportional to its concentration as it is described in the first term. Here $k_{\text{prod}}^{\text{Inh}}$ is the translation rate. The next two terms consider an uptake of the cytoplasmic inhibitor into the nucleus with an uptake rate $k_{\text{up}}^{\text{Inh}}$ and an export of the nuclear inhibitor into the cytoplasm with an export rate $k_{\text{ex}}^{\text{Inh}}$. We assume that also a degradation of the inhibitor takes place. This is described by the last term. The factor $k_{\text{deg}}^{\text{Inh}}$ represents the rate of degradation.

3.3 Nuclear inhibitor

We assume that the cytoplasmic inhibitor is taken up into the nucleus with an uptake rate $k_{\text{up}}^{\text{Inh}}$ and exported from the nucleus into the cytoplasm with an export rate $k_{\text{ex}}^{\text{Inh}}$, as described in the following,

$$\frac{dx_{14}}{dt} = k_{\text{up}}^{\text{Inh}} x_{13} - k_{\text{ex}}^{\text{Inh}} x_{15} \quad (16)$$

Nuclear inhibitor inhibits synthesis of TNF α -mRNA. This contribution is considered by the last term equation of eq. (8). We assume that a decrease of the mRNA synthesis is proportional to the nuclear inhibitor concentration. Thus, the factor k_{inh} represents the inhibition rate of TNF α -mRNA synthesis.

Table 1: Overview of the parameters used within the model

Parameter	value	unit	comment	description
k_{act}	0.31457 ± 0.03	$10^{-2} \mu\text{M} s^{-1}$	Fitted	activation rate of I κ B-Kinase
k_{inact}	0.29869 ± 0.03	s^{-1}	Fitted	inactivation rate of I κ B-Kinase
$k_{\text{ass}}^{\text{NI}}$	0.05 ± 0.03	$10^2 \mu\text{M}^{-1} s^{-1}$	Hoffmann et al.	rate of NF κ B I κ B association (cytosol)
$k_{\text{deg}}^{\text{NI}}$	$2 \cdot 10^{-5} \pm 10^{-5}$	s^{-1}	Pando and Verma	constitutive degradation rate of complex bound I κ B
k_{up}^{N}	0.83076 ± 0.2	s^{-1}	Fitted	uptake rate of NF κ B into the nucleus
k_{ex}^{N}	0.01972 ± 0.01	s^{-1}	Fitted	export rate of nuclear NF κ B
$k_{\text{prex}}^{\text{mT}}$	0.05595 ± 0.0095	s^{-1}	Fitted	formation/export rate of TNF α -mRNA
$k_{\text{deg}}^{\text{mT}}$	0.07541 ± 0.001	s^{-1}	Fitted	rate of TNF α -mRNA degradation
$k_{\text{prex}}^{\text{mI}}$	0.79136 ± 0.001	s^{-1}	Fitted	formation/export rate of I κ B-mRNA
$k_{\text{deg}}^{\text{mI}}$	0.18514 ± 0.001	s^{-1}	Fitted	rate of I κ B-mRNA degradation
$k_{\text{prod}}^{\text{I}}$	$0.49294 \pm 6 \cdot 10^{-4}$	s^{-1}	Fitted	translation rate of I κ B-mRNA
$k_{\text{deg}}^{\text{I}}$	$10^{-4} + 0.001$	s^{-1}	Pando and Verma	rate of constitutive I κ B degradation
$k_{\text{prod}}^{\text{T}}$	0.29276 ± 0.002	s^{-1}	Fitted	translation rate of TNF α -mRNA
k_{T}	0.02197 ± 10^{-4}	s^{-1}	Fitted	rate of soluble TNF α TNFR association
k_{up}^{I}	0.05246 ± 0.001	s^{-1}	Fitted	uptake rate of I κ B into the nucleus
k_{ex}^{I}	0.0297 ± 0.004	s^{-1}	Fitted	export rate of nuclear I κ B
$k_{\text{ass}}^{\text{mNI}}$	0.68769 ± 0.03	$10^2 \mu\text{M}^{-1} s^{-1}$	Fitted	rate of NF κ B I κ B association (nucleus)
$k_{\text{ex}}^{\text{NI}}$	0.10853 ± 0.06	s^{-1}	Fitted	export rate of nuclear NF κ B/I κ B
k_{tace}	0.03928 ± 0.003	no unit	Fitted	amount of transmembrane TACE
v_{TACE}	3.09988 ± 0.25	s^{-1}	Fitted	maximal conversion rate of TACE
K_{TACE}	0.21809 ± 0.03	$10^{-2} \mu\text{M}$	Fitted	Michaelis Menten constant of TACE
v_{IKK}	0.04471 ± 10^{-4}	s^{-1}	Fitted	maximal conversion rate of I κ k
K_{IKK}	0.50296 ± 0.01	$10^{-2} \mu\text{M}$	Fitted	Michaelis Menten constant of I κ k
$k_{\text{deg}}^{\text{mInh}}$	0.01237 ± 0.002	s^{-1}	Assumption	rate of inhibitor-mRNA degradation
$k_{\text{prex}}^{\text{mInh}}$	$6.05 \cdot 10^{-5} \pm 10^{-5}$	s^{-1}	Assumption	formation/export rate of inhibitor-mRNA
$k_{\text{deg}}^{\text{Inh}}$	0.01093 ± 0.0025	s^{-1}	Assumption	rate of inhibitor degradation
$k_{\text{prod}}^{\text{Inh}}$	0.00606 ± 0.0025	s^{-1}	Assumption	translation rate of inhibitor-mRNA
$k_{\text{up}}^{\text{Inh}}$	$0.00427 \pm 2 \cdot 10^{-5}$	s^{-1}	Assumption	uptake rate of inhibitor into the nucleus
$k_{\text{ex}}^{\text{Inh}}$	$1.59 \cdot 10^{-4} \pm 0.001$	s^{-1}	Assumption	export rate of nuclear inhibitor
k_{inh}	4.3935 ± 0.2	s^{-1}	Assumption	inhibitor rate of TNF α -mRNA synthesis

4 Simulation results

To simulate the model, the software Berkley MADONNA was used. The program code is listed in the appendix.

4.1 Initial conditions and a steady state

As the first step we perform simulations for different initial values and obtain the equilibrium after 10000 minutes of simulation time. We find numerically the steady state of an inactivated system, i.e. the system with the LPS activation coefficient $k_{\text{act}} = 0$. The only restriction for the initial values is, that the sum of all NF κ B concentrations has to be fixed (remember that NF κ B may exist free or complex bound, as well as nuclear or cytoplasmic). This restriction comes from the assumption that the overall concentration of NF κ B remains constant, which is in agreement with the assumptions of Lipniacki et al. The overall concentration is set to $0.06\mu\text{M}$, which is a typical NF κ B concentration in fibroblasts [5]. But we suppose that NF κ B concentration in macrophages is of the same order of magnitude. It turned out that a single steady state exist for the system. This is exemplary shown in Fig.2, where the time course of nuclear NF κ B is plotted. As we see, the concentration reaches a steady state. The steady state values are listed for all fourteen states in Tab. 2. For further simulations we use these values as initial values.

4.2 Comparison of model prediction and measured TNF α

To test the model's ability to describe TNF α production, the parameters were varied in order to fit the model curve to a set of data points. The result of this is shown in Fig.3. As we see, the qualitative behaviour is well described, even though a distinct shift is visible between measurement and model curve. This shows the limitation of our model. The model does not consider explicitly any time delay between the activation of the cell and the production of TNF α -mRNA and TNF α protein. Also the transport of TNF α and its anchoring to the membrane is not taken into consideration so far. Moreover there are no diffusion or transport processes in the cytoplasm considered. We can easily imagine that these processes require a certain time, which

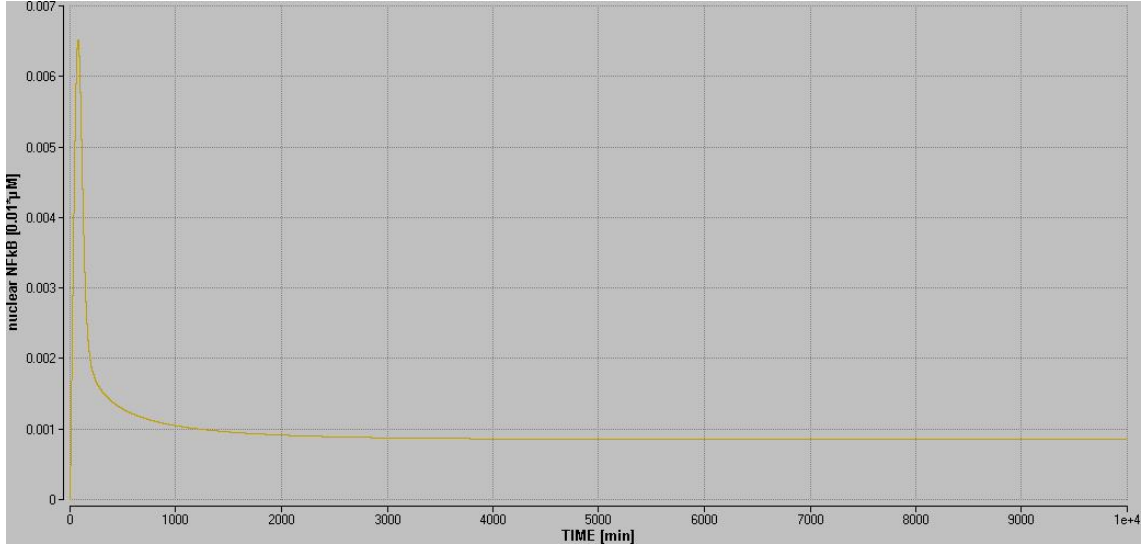


Figure 2: Nuclear NF κ B reaches its steady state

Table 2: **Overview of the states used within the model and the steady state values**

state	steady state value	unit	description
x_1	0	$10^{-2} \mu\text{M}$	activated I κ k
x_2	5.9981	$10^{-2} \mu\text{M}$	cytoplasmic NF κ B/I κ B complex
x_3	$1.582 \cdot 10^{-4}$	$10^{-2} \mu\text{M}$	cytoplasmic NF κ B
x_4	0.15442	$10^{-2} \mu\text{M}$	cytoplasmic I κ B
x_5	$6.428 \cdot 10^{-4}$	$10^{-2} \mu\text{M}$	nuclear NF κ B
x_6	0.002747	$10^{-2} \mu\text{M}$	I κ B mRNA
x_7	$6.9273 \cdot 10^{-4}$	$10^{-2} \mu\text{M}$	TNF α mRNA
x_8	$3.4218 \cdot 10^{-4}$	$10^{-2} \mu\text{M}$	cellular TNF α
x_9	0.00946	$10^{-2} \mu\text{M}$	soluble TNF α
x_{10}	0.26868	$10^{-2} \mu\text{M}$	nuclear I κ B
x_{11}	0.00109	$10^{-2} \mu\text{M}$	nuclear NF κ B/I κ B complex
x_{12}	$3.143 \cdot 10^{-6}$	$10^{-2} \mu\text{M}$	Inhibitor-mRNA
x_{13}	$1.721 \cdot 10^{-5}$	$10^{-2} \mu\text{M}$	Inhibitor
x_{14}	0	$10^{-2} \mu\text{M}$	nuclear inhibitor

cause that the secretion of $\text{TNF}\alpha$ starts with the observed delay.

We may assume that the most time-consuming steps in this process are the synthesis of $\text{TNF}\alpha$ -mRNA and the production, transport, and cleavage of $\text{TNF}\alpha$ protein. The functions which describe the concentration of $\text{TNF}\alpha$ -mRNA (x_7) and soluble $\text{TNF}\alpha$ protein (x_9) should therefore also depend on a time delay T , i.e. $x_7(t) = f(t - T_1)$ and $x_9(t) = f(t - T_2)$. It is not necessary to explicitly model these delays because x_7 and x_9 have no influence on the preceding states of the system (see section 6.2 for an approach on an explicit delay modelling). Because of this, we may add the occurring delays and shift the time course of x_9 so that the secretion of $\text{TNF}\alpha$ occurs later. This was made in Fig.4. Here we shifted x_9 about 30 minutes away from the origin. As we see, the shifted measurements are better described by the model.

In order to further minimize the deviation between model curve and data points we carried out a parameter estimation with the optimization tool MUSCOD-II, which allows to quickly implement and solve optimal control problems in differential-algebraic equations (for a brief introduction in using MUSCOD-II see [7]). Here, MUSCOD found the optimal parameter values which minimize the deviation between model curve and data points, i.e. it found the best possible fit of the model curve to the set of data points. The result is shown in Fig.5. The optimized parameter values are listed in Tab. 1. As we see, there are still some deviations remaining. These may be explained by inaccuracies in the measuring process. On the other hand they may still attribute to simplifications we made in the model, as we mentioned above.

4.3 Time courses of all fourteen states

In this section the time courses after LPS stimulation at time zero are shown for all fourteen states. So far, we have no quantitative experimental data to validate our model. However, Dr. A. Gratchev is currently performing in his laboratory experiments, which should give us the missing data. We expect that using these data we can validate the model, both quantitatively (doing numerical parameter estimation) and qualitatively.

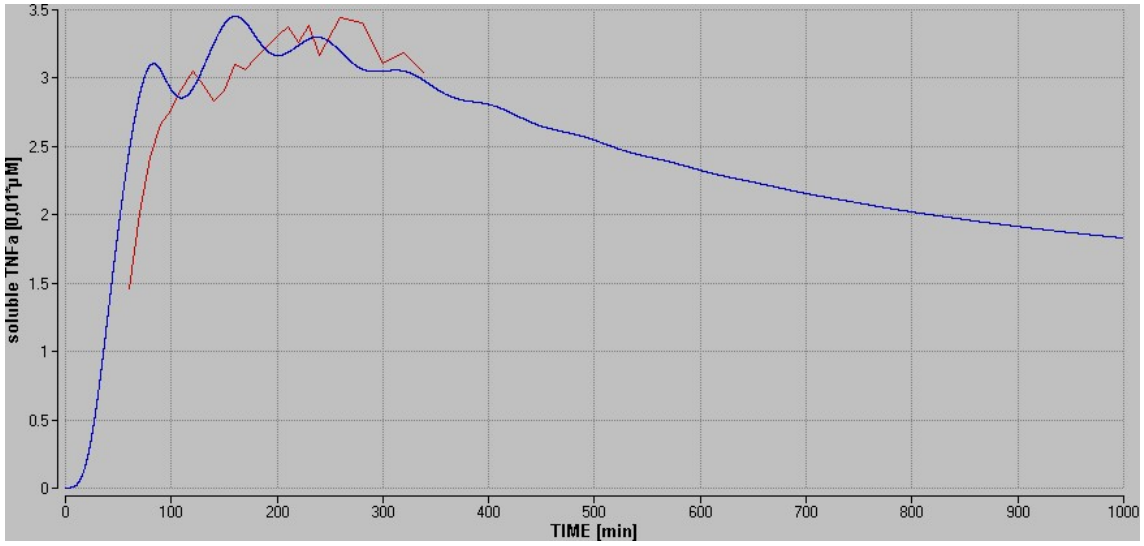


Figure 3: Comparison of model prediction and measured TNF α

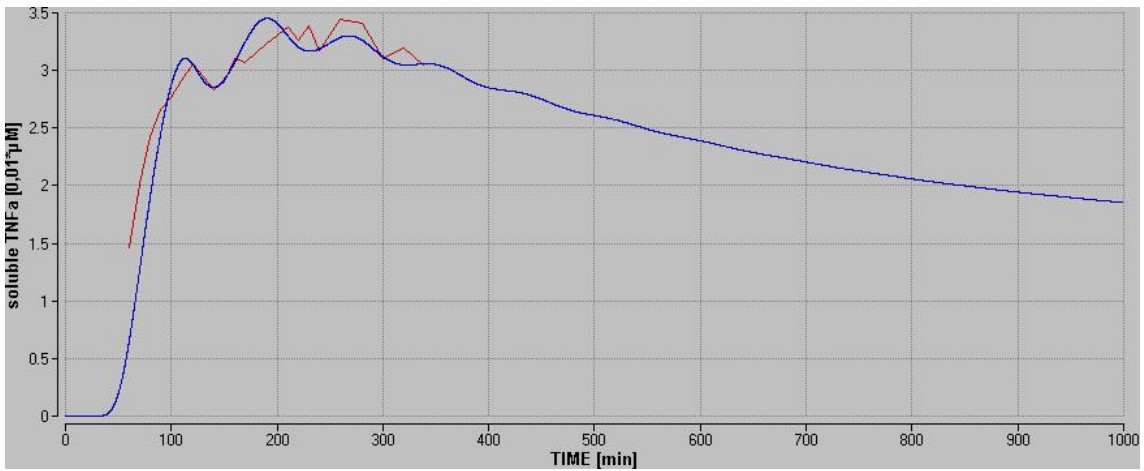


Figure 4: Comparison of model prediction and shifted measurements

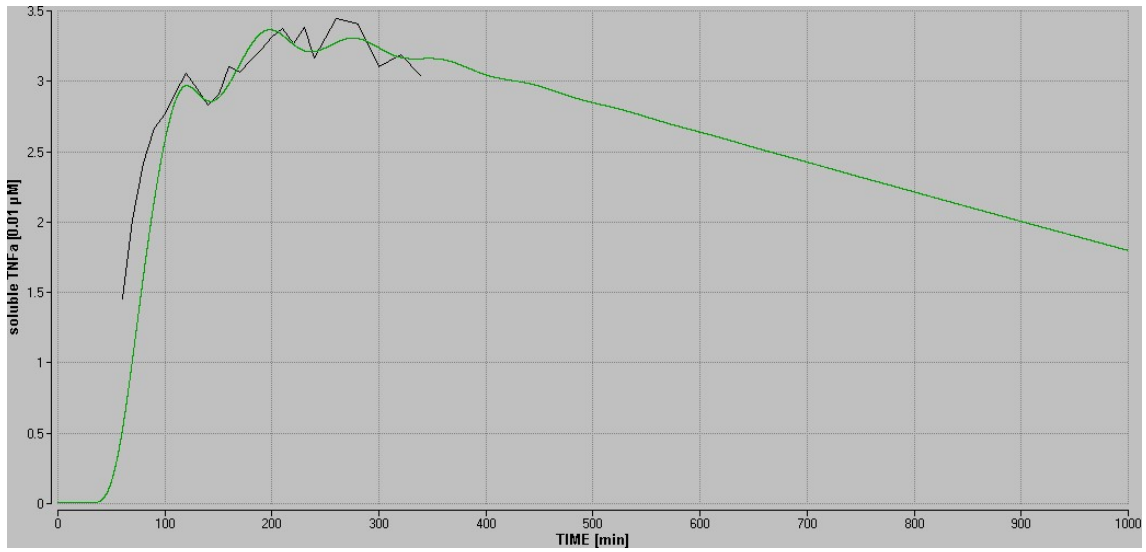


Figure 5: Time course of the model using optimized parameter values

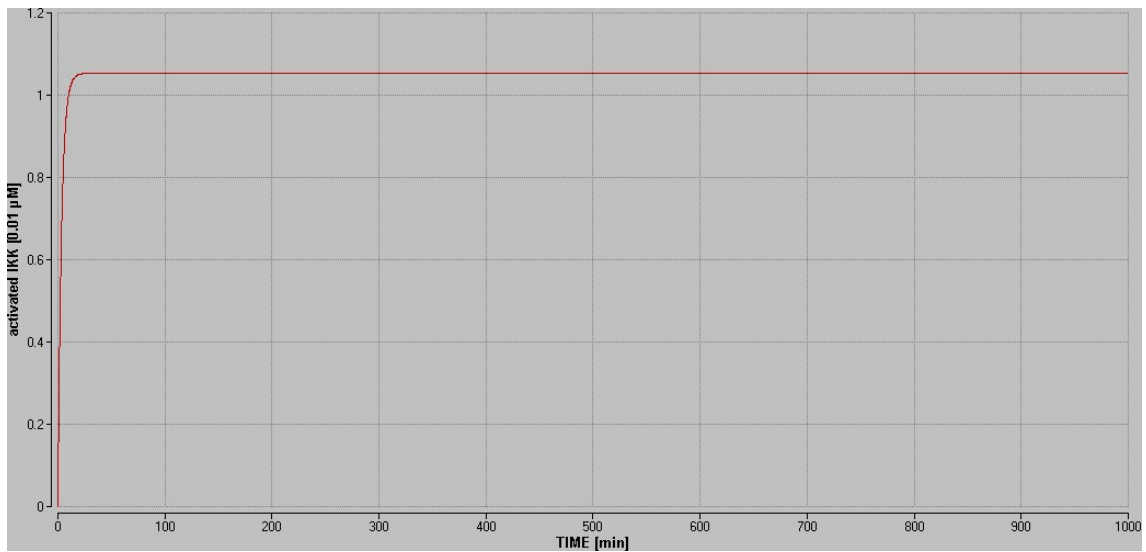


Figure 6: Time course of $I\kappa K$ concentration after activation at time zero

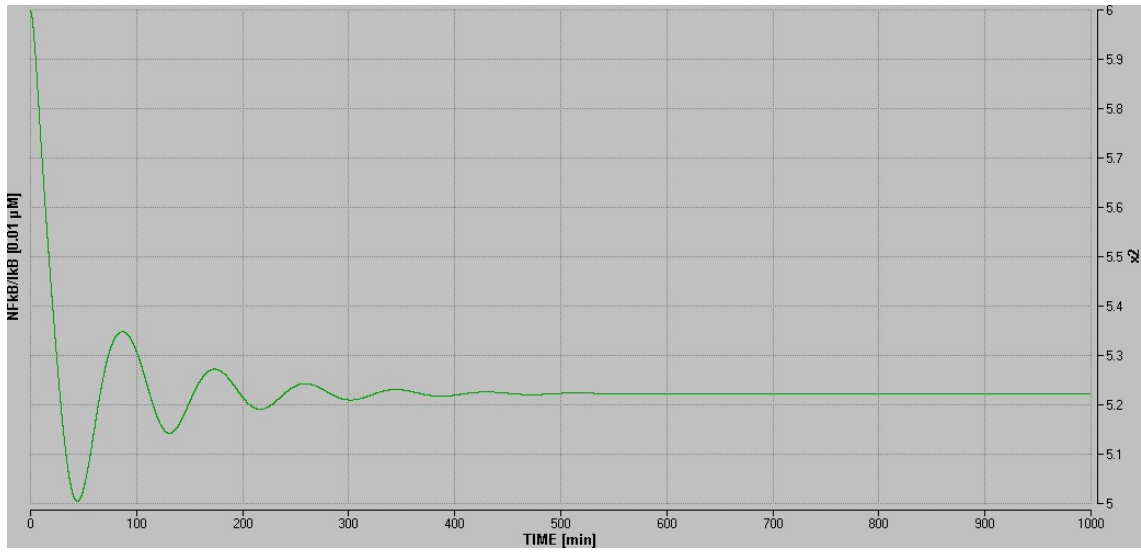


Figure 7: Time course of cytoplasmic $\text{NF}\kappa\text{B}/\text{I}\kappa\text{B}$ concentration

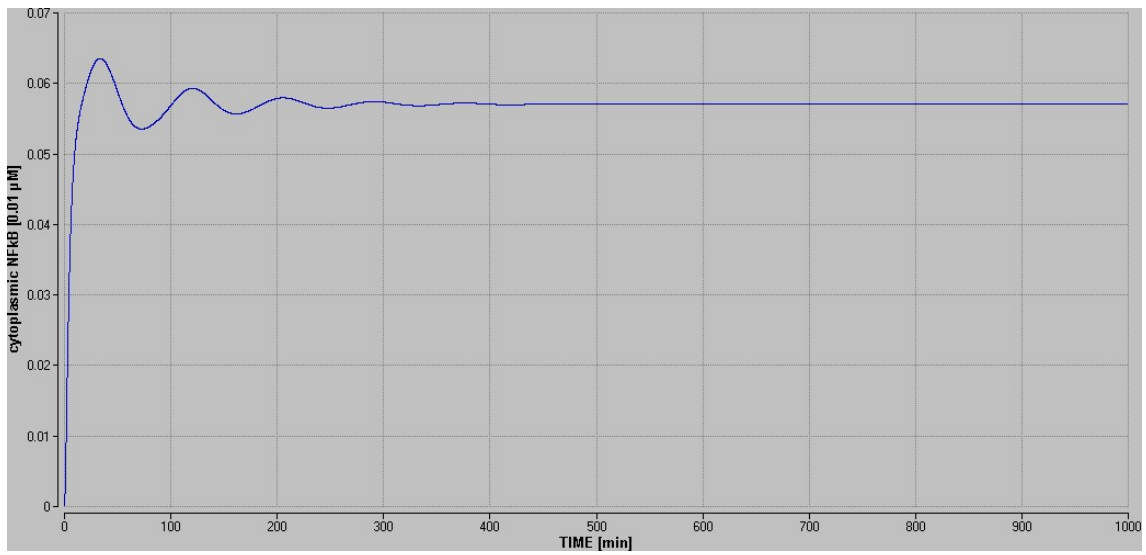


Figure 8: Time course of cytoplasmic $\text{NF}\kappa\text{B}$ concentration

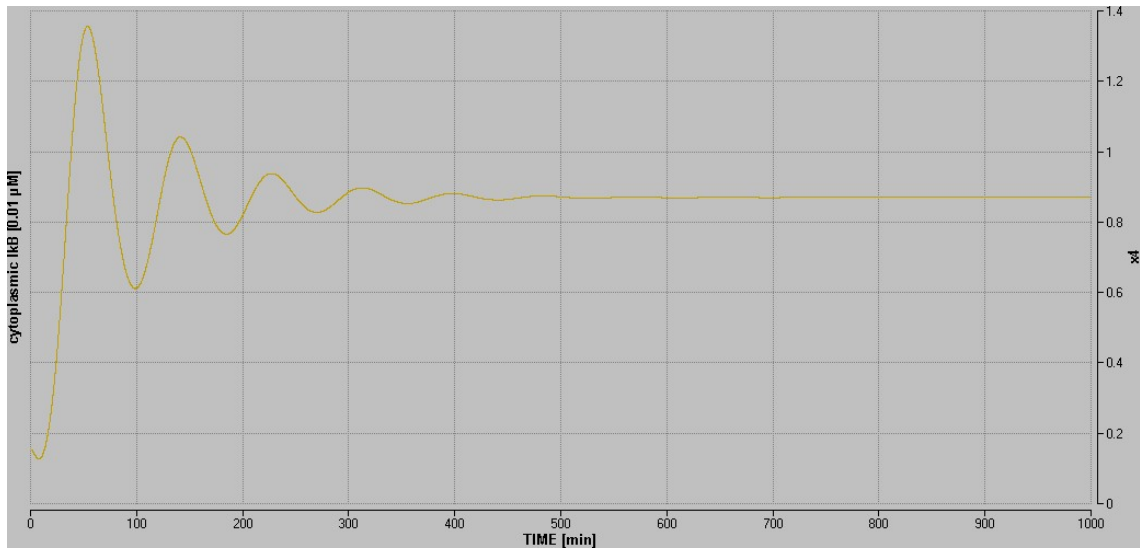


Figure 9: Time course of cytoplasmic $I\kappa B$ concentration

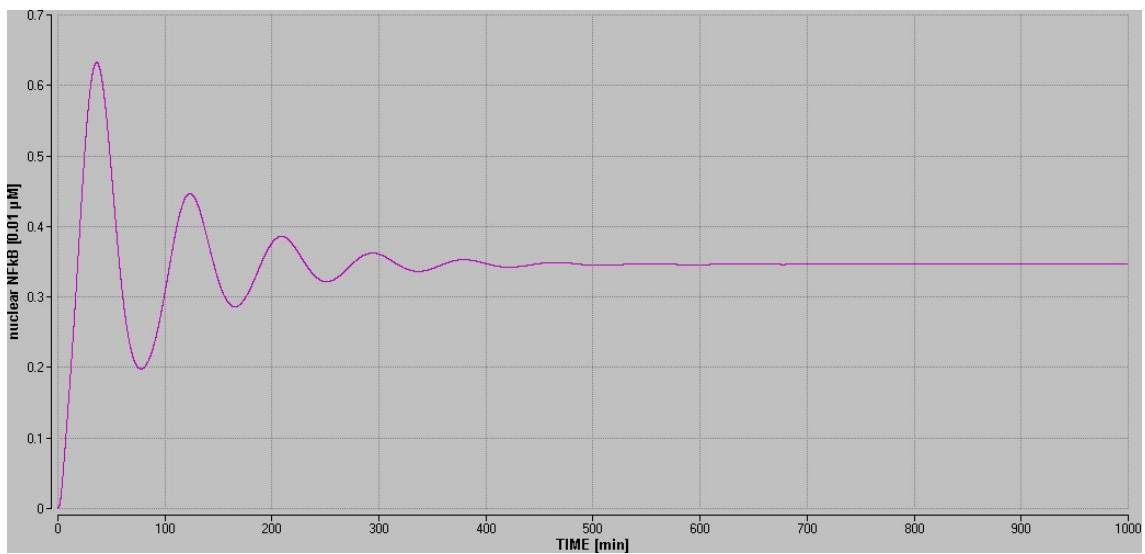


Figure 10: Time course of nuclear $NF\kappa B$ concentration

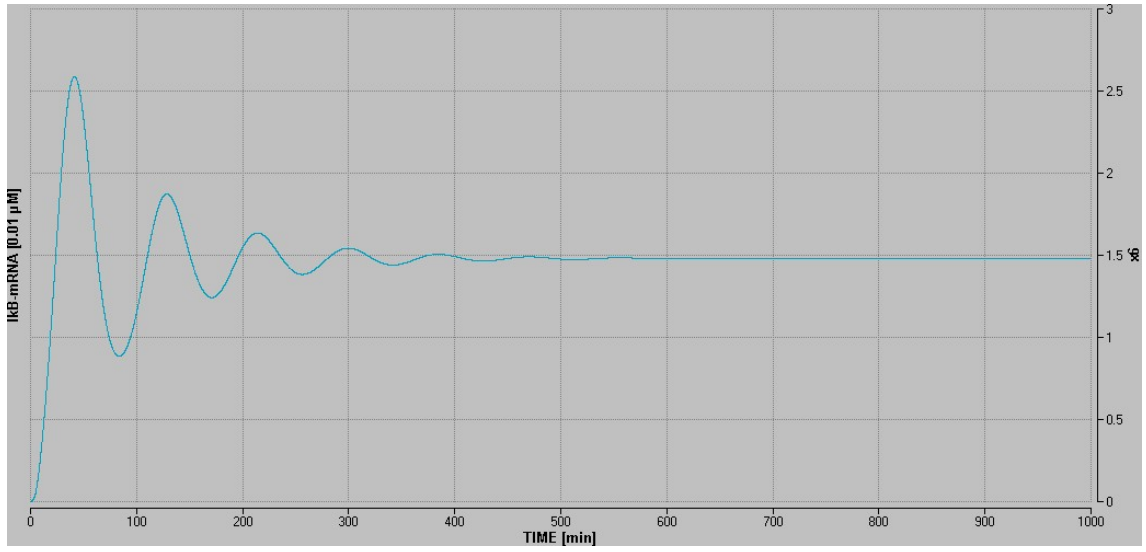


Figure 11: Time course of $I\kappa B$ -mRNA concentration

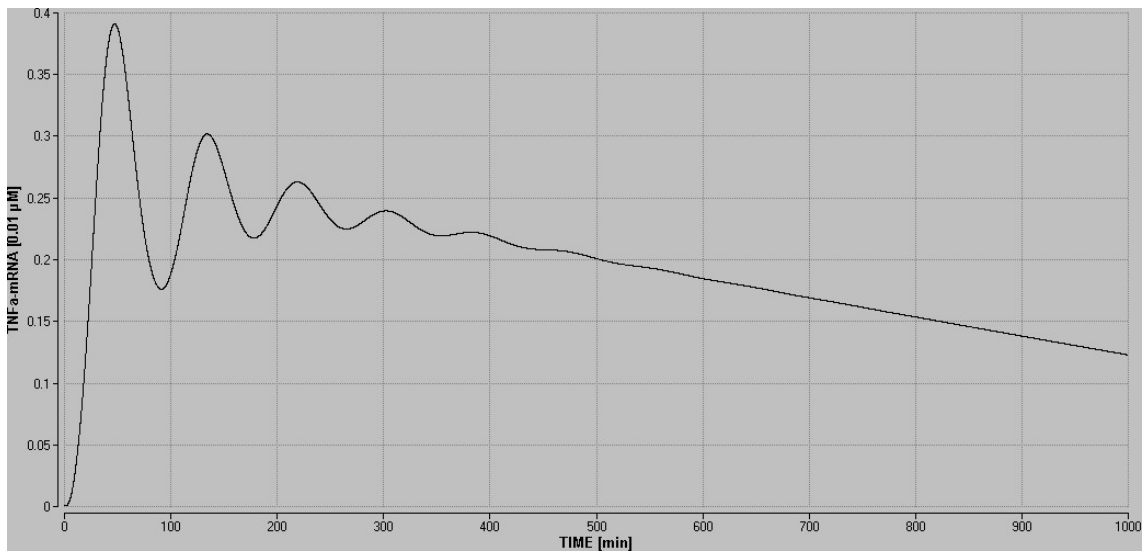


Figure 12: Time course of $TNF\alpha$ -mRNA concentration

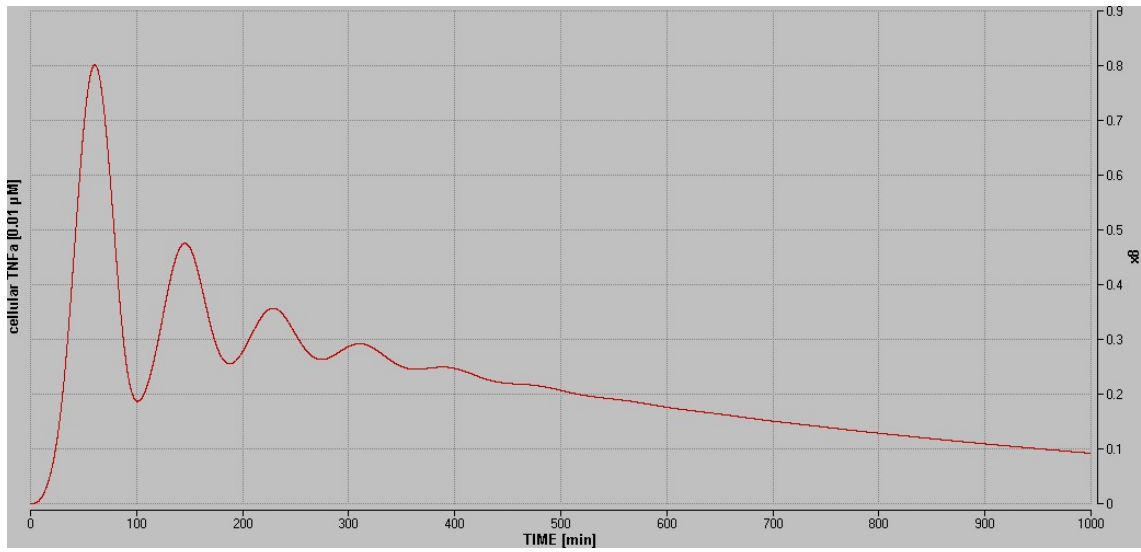


Figure 13: Time course of cellular TNF α concentration

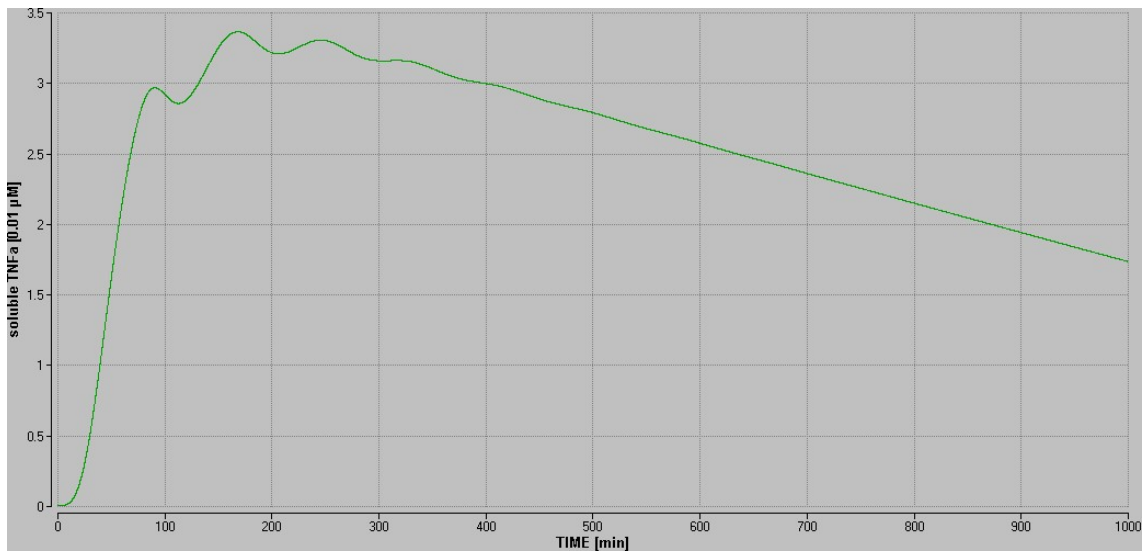


Figure 14: Time course of soluble TNF α concentration

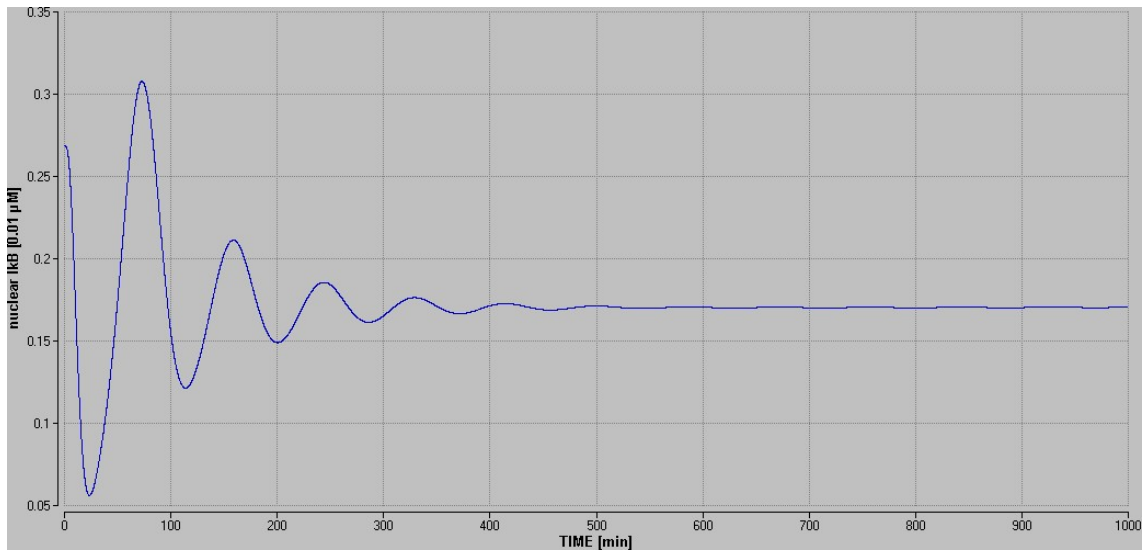


Figure 15: Time course of nuclear $I\kappa B$ concentration

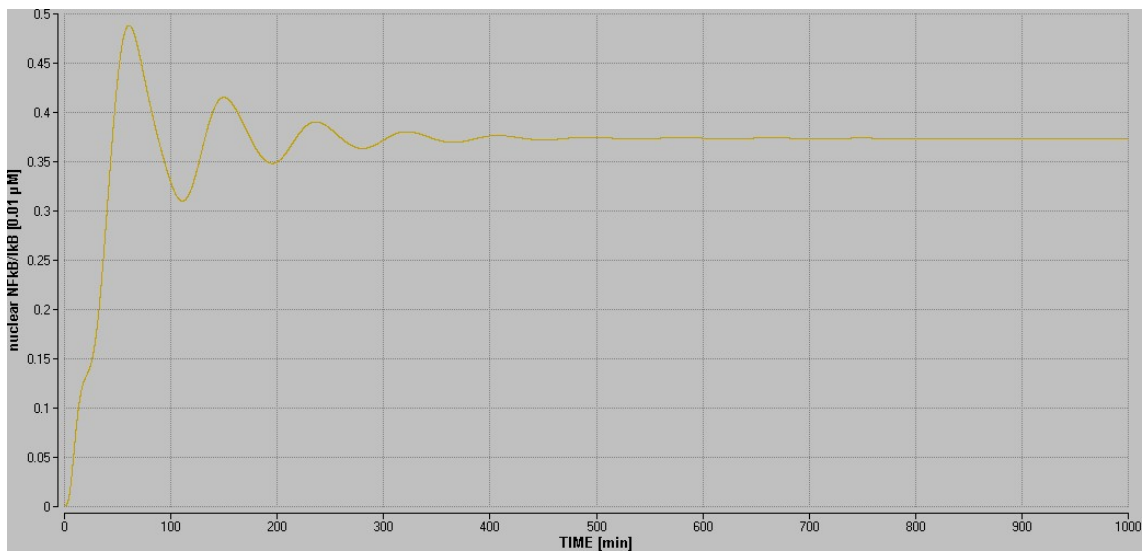


Figure 16: Time course of nuclear $NF\kappa B/I\kappa B$ concentration

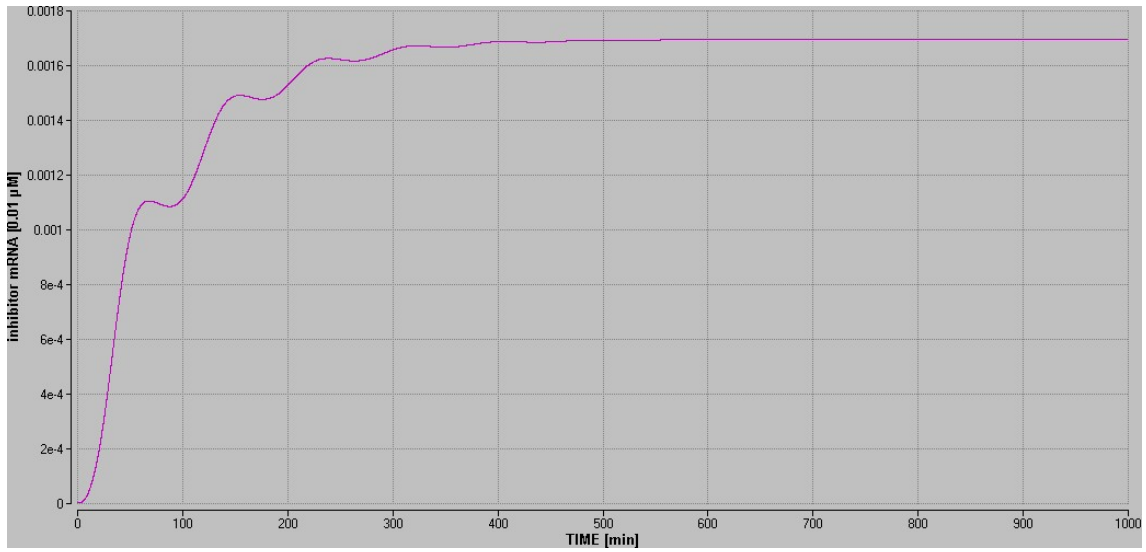


Figure 17: Time course of inhibitor-mRNA concentration

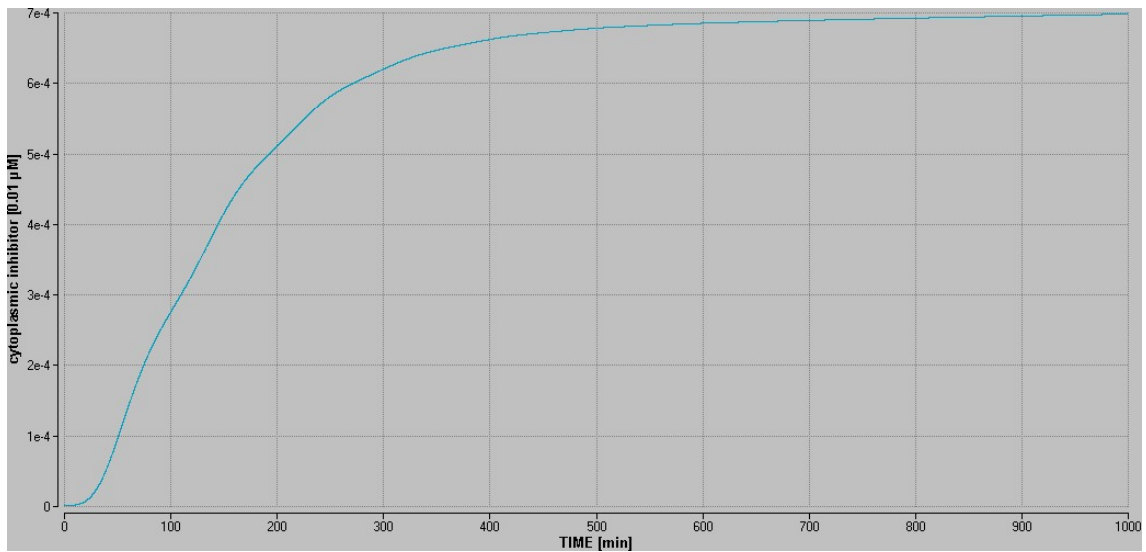


Figure 18: Time course of cytoplasmic inhibitor concentration

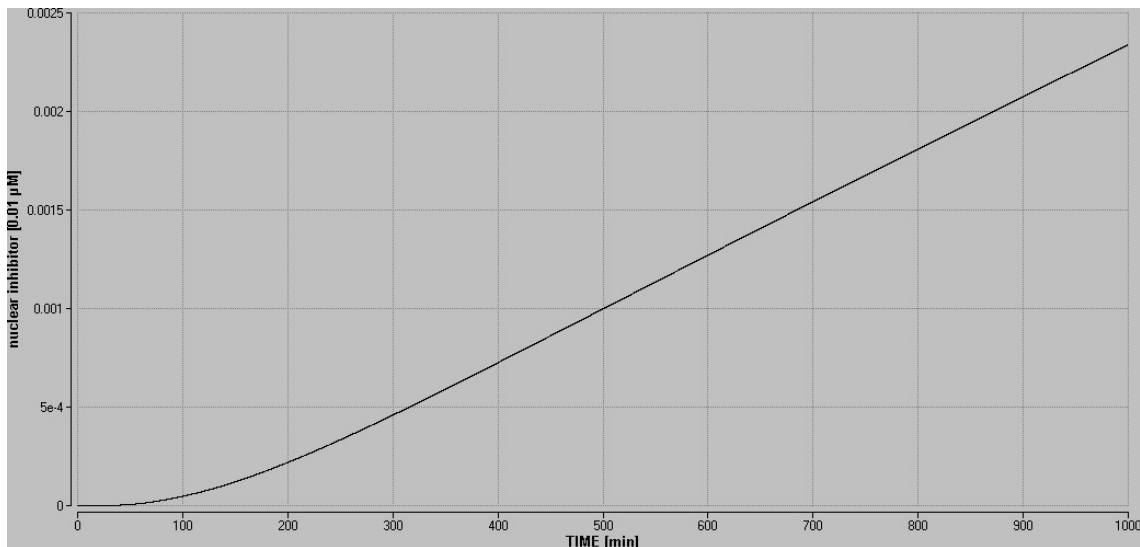


Figure 19: Time course of nuclear inhibitor concentration

5 Conclusions and outlook

The simulations show that the hypothetically inhibitor functions in the way confirmed by experiments. It inhibits the secretion of $\text{TNF}\alpha$, which decreases in spite of the constant stimulation with LPS. The same time, the concentration of $\text{NF}\kappa\text{B}$ stays constant. However, numerical simulations of the model with different assumptions about the inhibitor show that many settings stay in agreement with the experimental observations. Further results are needed to validate the different hypotheses. The prior work to do in the future is, therefore, to gain more experimental data. In the present work, only the time course of soluble $\text{TNF}\alpha$ is considered. As we see in section 4.2, the qualitative behaviour of $\text{TNF}\alpha$ secretion may be described when we shift the soluble $\text{TNF}\alpha$ about 30 minutes away from the origin. This can be justified by the fact, that transport processes have been neglected. Even if some aberrations remain, the result may indicate that the assumptions we made to model the LPS induced $\text{TNF}\alpha$ secretion include the most critical steps of the process. The observed aberrations are not too strong and may be caused by measuring errors and simplifications in the model. The present model is only a first step in an attempt to understand the regulation of LPS induced $\text{TNF}\alpha$ secretion. Future measurements, i.e. $\text{NF}\kappa\text{B}$, $\text{I}\kappa\text{B}$ and $\text{TNF}\alpha$ -mRNA time courses, will clarify whether the model already

reflects the real conditions in the cell. Having these measurements, further parameter estimations with MUSCOD will probably lead to better results. A working model for $\text{TNF}\alpha$ secretion will certainly represent a strong support for research in the regulation of LPS response system. Even the present model is used to get evidence on the function of the hypothetical inhibitor. The model helps to establish new experiments and increases the notion of the complex process.

Acknowledgements

This work was supported by Dr. M. Diehl and A. Boltz, who supported especially in parameter estimation with MUSCOD, Dr. A. Gratchev, who provided the experimental data, and Dr. A. Marciniak-CZochra, who gave support in the modelling process.

References

- [1] Janeway et al. *Immunology*, 5th edition
- [2] Palsson-Mcdermott E, O'Neil J: *Signal transduction by the lipopolysaccharide receptor, Toll like receptor 4*, *Immunology* 113 (2004), 153-162
- [3] Gilmore T, *The Rel/NF-kappaB Signal Transduction Pathway*, <http://www.nf-kb.org> (2004)
- [4] Takeda K, Shizuo A: *Toll receptors and pathogen resistance*, *Cellular Microbiology* (2003) 5(3), 143-153
- [5] Hoffmann H, Levchenko A, Martin LS, Baltimore D. *The I κ B-NF- κ B Signaling Module: Temporal Control and Selective Gene Activation*, *Supplement 2 Parameter Determination Science* (2002) Vol 298 page 1241-43.
- [6] Lipniacki T, Paszek P, Brasier A, Luxon B, Kimmel M: *Mathematical model of NF- κ B regulatory model*, *Journal of Theoretical Biology*, 228 (2004) 195-215 and references therein.
- [7] Alberts et al. *molecular biology of the cell*, 4th edition, p898f.

- [8] Diehl M, Leineweber D, Schaefer A. *Muscod-II Users' Manual*, Preprint 2001-25, June (2001) .

6 Appendix

6.1 MADONNA

{Secretion model}

METHOD RK4

STARTTIME=0 {h}

STOPTIME=2000 {h}

DT = 0.01

DTMAX = 0.05

{Mass balances}

$d/dt(x1) = kact - kinact * x1$

$d/dt(x2) = -x1 * IKK + kassNI * x3 * x4 + kexNI * x11 - kdissNI * x2$

$d/dt(x3) = x1 * IKK - kassNI * x3 * x4 + kexN * x5 - kupN * x3 + kdissNI * x2$

$d/dt(x4) = -kassNI * x3 * x4 + kprodI * x6 - kupI * x4 + kexI * x10 - kdegI * x4 - IKK2 * x1$

$d/dt(x5) = kupN * x3 - kexN * x5 - kassnNI * x10 * x5 + kdissNI * x11$

$d/dt(x6) = kprodmI * x5 - kdegmI * x6$

$d/dt(x7) = kprodmT * x5 - kdegmT * x7 - kinh * x14$

$d/dt(x8) = kprodT * x7 - ktace * TACE$

$d/dt(x9) = ktace * TACE - kT * x9$

$d/dt(x10) = x4 * kupI - x10 * kexI - kassnNI * x10 * x5$

$d/dt(x11) = kassnNI * x10 * x5 - kexNI * x11 - kdissNI * x11$

{Hypothetical inhibitor}

$d/dt(x12) = kprodmInh * x5 - kdegmInh * x12$

$d/dt(x13) = kprodInh * x12 - kupInh * x13 + kexInh * x14 - kdegInh * x13$

$d/dt(x14) = kupInh * x13 - kexInh * x14$

{Kinetics}

$TACE = VTACE * x8 / (KTACE + x8)$

$IKK = VIKK * x2 / (KIKK + x2)$

$IKK2 = VIKK * x4 / (KIKK + x4)$

{System parameter}

kact=0

kinact=1

kassNI=0.25

kupN=1

kexN=0.001

kprodT=0.1

kdegmT=0.1

kprodI=1.2

kdegmI=0.5

kprodI=0.25

kprodT=0.5

kT=0.25

kupI=0.2

kexI=0.2

kassnNI=0.75

kexNI=1.4

ktace=0.9

kprodInh=0.001

kdegmInh=0.0001

kprodInh=0.001

kupInh=0.0001

kexInh=0.0001

kinh=0.002

kdegInh=0.001

kdegI=0.001

kdissNI=0.00002

VTACE=2

KTACE=0.5

VIKK=0.24

KIKK=0.5

{Initial values}

init x1 = 0

init x2 = 5.9981022087454425E+00

```
init x3 =1.5818826398096992E-04
init x4 =1.5442188244993038E-01
init x5 =6.4275790734671262E-04
init x6 =2.7472942804603008E-03
init x7 =6.9271355198135198E-04
init x8 =3.4217913586747923E-04
init x9 =9.4550791345240949E-03
init x10 =2.6868168730520087E-01
init x11 =1.0940040832671408E-03
init x12 =3.1434441167159540E-06
init x13 =1.7207426188000975E-06
init x14 =0
```

```
{Bounds}
```

```
limit x1>=0
limit x2>=0
limit x3>=0
limit x4>=0
limit x5>=0
limit x6>=0
limit x7>=0
limit x8>=0
limit x9>=0
limit x10>=0
limit x11>=0
limit x12>=0
limit x13>=0
limit x14>=0
```

6.2 Modelling a time delay

In order to model a time delay we consider a small area around the nucleus which is divided into several compartments of the same volume. Newly synthesized $\text{TNF}\alpha$ -mRNA has to pass through all these compartments before it may be translated by ribosomes. In fact it is not the movement of mRNA through the cytoplasm which is the time-consuming step, but the process of mRNA-synthesis. Therefore, the follow-

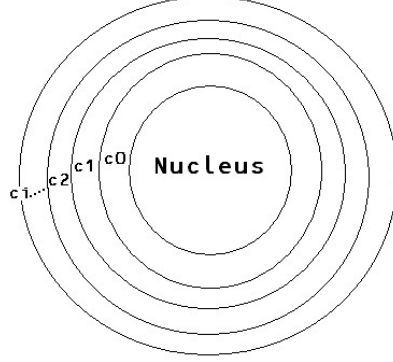


Figure 20: A small area around the nucleus is divided into compartments

ing approach does not reflect the real biological circumstances. However, the outcome would be the same even if we would try to model the real biological events: TNF α -mRNA will be available for translation only after a delay T . We use eq. (8) to model the dynamics of mRNA synthesis and the transport in the first compartment. The mRNA concentrations in the compartments are denoted by c_i , where c_0 is the mRNA concentration in the first compartment. Next we assume that the mRNA-molecules undergo a directed movement from one compartment to the next with a constant velocity v , with $v = \frac{L}{T}$, where T is the delay and L is the radial length of the considered area around the nucleus. In this case, the flux of mRNA molecules from one compartment to the other should be proportional to the gradient in concentration between the compartments. The change of TNF α -mRNA concentration is then described by,

$$\frac{dc_i}{dt} = -v \cdot \nabla c_i \quad (17)$$

If we consider a one dimensional case we can approximate the gradient and rewrite eq. (17),

$$\frac{dc_i}{dt} = -v \frac{dc_i}{dx} \approx -v \frac{c_i - c_{i-1}}{\Delta x}, \text{ with } i = 1, \dots, N \quad (18)$$

If we insert $\Delta x = \frac{L}{N}$ and $v = \frac{L}{T}$ we obtain:

$$\frac{dc_i}{dt} = -v \frac{c_i - c_{i-1}}{\Delta x} = -N \frac{c_i - c_{i-1}}{T} \quad (19)$$

If we consider three compartments (N=2) we obtain the following equations:

$$\frac{dc_0}{dt} = k_{\text{prex}}^{\text{mT}}x_5 - k_{\text{deg}}^{\text{mT}}x_7 - k_{\text{inh}}x_{14}, \quad (20)$$

$$\frac{dc_1}{dt} = -2\frac{c_1 - c_0}{T}, \quad (21)$$

$$\frac{dc_2}{dt} = -2\frac{c_2 - c_1}{T} \quad (22)$$

The synthesis of TNF α is then proportional to the mRNA concentration in the last compartment (c_2),

$$\frac{dx_8}{dt} = k_{\text{prod}}^{\text{T}}c_2 - k_{\text{tace}}v_{\text{TACE}}\frac{c_2}{K_{\text{TACE}} + x_8} \quad (23)$$

6.3 MUSCOD

6.3.1 c-File

```

/*
 * MUSCOD-II/BIOOPT/SRC/LSQ_neu.c
 * (c) Stefan Quint, 2005
 */
#include <math.h>
#include "def_usrmod.h"
#include "def_ind.h"
#define NMOS 26
#define NP 32
#define NRC 0
#define NRCE 0
#define NXD 14
#define NXA 0
#define NU 0
#define NPR 0
#define NRD_S 0
#define NRDE_S 0

/*static double messwerte0[25]={-1,1.457379301,2.014416141,2.420053453,2.665505764,2.768474345,
2.913948619,3.053305108,2.943387058,2.832130278,2.90513942,3.101322838,3.065282054,3.14963376,
3.222649878,3.308669116,3.376885565,3.262475717,3.383114547,3.167825944,3.442518362,3.408076287,
3.104333681,3.18910227,3.032389547};
*/

```

```

static double messwerte0[25]={-1,-1,-1,-1,2.665505764,2.768474345,2.913948619,3.053305108,
2.943387058,2.832130278,2.90513942,3.101322838,3.065282054,3.14963376,3.222649878,
3.308669116,3.376885565,3.262475717,3.383114547,3.167825944,3.442518362,3.408076287,3.104333681,
3.18910227,3.032389547};

static void rhsfcn(double *t, double *xd, double *xa, double *u,double *p,
double *rhs, double *rwh, long *iwh, long *info, double TR)
{
double x1,x2,x3,x4,x5,x6,x7,x8,x9,x10,x11,x12,x13,x14,x1_d,x2_d,x3_d,x4_d,x5_d,x6_d,x7_d,x8_d,x9_d,
x10_d,x11_d,x12_d,x13_d,x14_d,k1,k2,k4,k5,k6,k7,k8,k9,k10,k11,k12,k13,k14,k15,k16,k17,k18,k19,k20,
k21,k22,k23,k24,k25,c6a,c5a,KM,V,Vi,KMi;

/* Umbenennung der Zustaeende */
x1=xd[0]; x2=xd[1]; x3=xd[2]; x4=xd[3]; x5=xd[4]; x6=xd[5];x7=xd[6]; x8=xd[7]; x9=xd[8];
x10=xd[9]; x11=xd[10]; x12=xd[11]; x13=xd[12]; x14=xd[13];
/* Parameter */
k1=p[0]; k2=p[1]; k4=p[2]; k5=p[3]; k6=p[4];k7=p[5];k8=p[6]; k9=p[7]; k10=p[8];k11=p[9];
k12=p[10];k13=p[11]; k14=p[12]; k15=p[13]; k16=p[14]; k17=p[15]; k18=p[16]; k19=p[17];
k20=p[18]; k21=p[19];k22=p[20]; k23=p[21]; k24=p[22]; k25=p[23]; c5a=p[24]; c6a=p[25];
V=p[26]; KM=p[27]; Vi=p[28]; KMi=p[29];
/* Gleichungen */
x1_d=TR*(k1-k2*x1);
x2_d=-x1*Vi *(x2/(KMi+x2))+k4*x3*x4+k17*x11-c6a*x2;
x3_d=x1*Vi *(x2/(KMi+x2))-k4*x3*x4+k6*x5-k5*x3+c6a*x2;
x4_d=-k4*x3*x4+k11*x6-k14*x4+k15*x10-c5a*x4-Vi *(x4/(KMi+x4))*x1;
x5_d=k5*x3-k6*x5-k16*x10*x5+c6a*x11;
x6_d=k9*x5-k10*x6;
x7_d=k7*x5-k8*x7-k24*x14;
x8_d=k12*x7-k18*V*(x8/(KM+x8));
x9_d=k18*V*(x8/(KM+x8))-k13*x9;
x10_d=x4*k14-x10*k15-k16*x10*x5;
x11_d=k16*x10*x5-k17*x11-c6a*x11;
x12_d=k19*x5-k20*x12;
x13_d=k21*x12-k22*x13 +k23*x14 -k25*x13;
x14_d=k22*x13-k23*x14;
/* Output (Gleiche Reihenfolge wie Zustaeende) */
rhs[0]=x1_d; rhs[1]=x2_d;rhs[2]=x3_d;rhs[3]=x4_d;rhs[4]=x5_d;rhs[5]=x6_d;rhs[6]=x7_d;
rhs[7]=x8_d;rhs[8]=x9_d;rhs[9]=x10_d;rhs[10]=x11_d;rhs[11]=x12_d;rhs[12]=x13_d;rhs[13]=x14_d;
};

```

```

static void ffcn0(double *t, double *xd, double *xa, double *u,
double *p, double *rhs, double *rwh, long *iwh, long *info)
{
rhsfcn(t,xd,xa,u,p,rhs,rwh,iwh,info, 0);
};

static void ffcn1(double *t, double *xd, double *xa, double *u,
double *p, double *rhs, double *rwh, long *iwh, long *info)
{
rhsfcn(t,xd,xa,u,p,rhs,rwh,iwh,info, 1);
};

static void lsqfcn(
double *ts, /* physical time (I) */
double *sd, /* differential state vector (I) */
double *sa, /* algebraic state vector (I) */
double *u, /* control vector (I) */
double *p, /* global model parameter vector (I) */
double *pr, /* local i.p.c. parameter vector (I) */
double *res, /* i.p.c. residual (0) */
long *dpnd, /* argument dependency code (I/0) */
long *info /* error code (0) */
)
/*
* decoupled or coupled interior point constraint (i.p.c.) residual
*/
{
int i=0;
long mstage;
double m1;

if (*dpnd) {
*dpnd = RFCN_DPND(*ts, *sd, *sa, *u, *p, *pr);
return;
}

m1=p[30]; /*Normierungsparameter fr die Messwerte */

get_cimos(&mstage);
for (i=0;i<2;i++){res[i]=0;}

```

```

    if (mstage!=0)
    {
    if (messwerte0[mstage-1]!=-1){
    res[0]=sd[8]/m1-messwerte0[mstage-1];
    };

    if (messwerte1[mstage-1]!=-1){
    res[1]=sd[6]/m1-messwerte1[mstage-1]; (sd-mess*m)/m <- als Gewicht
    };
    };
    };

static void lsqfcn1(
    double *ts, /* physical time (I) */
    double *sd, /* differential state vector (I) */
    double *sa, /* algebraic state vector (I) */
    double *u, /* control vector (I) */
    double *p, /* global model parameter vector (I) */
    double *pr, /* local i.p.c. parameter vector (I) */
    double *res, /* i.p.c. residual (0) */
    long *dpnd, /* argument dependency code (I/0) */
    long *info /* error code (0) */
)
{
    int i;
    double w;
    if (*dpnd) {
        *dpnd = RFCN_DPND(*ts, *sd, *sa, *u, *p, *pr);
        return;
    }

    w=p[31];
    res[0 ]=p[0] - 6.1722098116373747E-01;
    res[1 ]=p[1] - 5.6980171668129942E-01;
    res[2 ]=p[2] - 0.05;
    res[3 ]=p[3] - 8.7830922168916425E-01;
    res[4 ]=p[4] - 1.0630476393773394E-01;
    res[5 ]=p[5] - 2.7348298925779746E-01;
    res[6 ]=p[6] - 4.1608054409330536E-01;

```

```

res[7 ]=p[7]   - 8.5152358946818307E-01;
res[8 ]=p[8]   - 2.2223472075535566E-01;
res[9 ]=p[9]   - 5.0944750147229892E-02;
res[10]=p[10]  - 3.4672142827355834E-01;
res[11]=p[11]  - 2.7704296865884957E-02;
res[12]=p[12]  - 5.1426686976272895E-02;
res[13]=p[13]  - 0.014;
res[14]=p[14]  - 0.69;
res[15]=p[15]  - 0.11;
res[16]=p[16]  - 0.043;
res[17]=p[17]  - 0.0001;
res[18]=p[18]  - 0.014;
res[19]=p[19]  - 0.0177;
res[20]=p[20]  - 0.00208;
res[21]=p[21]  - 0.00301;
res[22]=p[22]  - 4.39314;
res[23]=p[23]  - 0.0101;
res[24]=p[24]  - 0.001;
res[25]=p[25]  - 2e-5;
res[26]=p[26]  - 3.1;
res[27]=p[27]  - 0.23;
res[28]=p[28]  - 0.045;
res[29]=p[29]  - 0.5;
res[30]=p[30]  - 9.5955236609350314E-01;

```

```

    for (i=0;i<31;i++){
res[i]=res[i]*w;
    }

```

```

};

```

```

void def_model(void)
{
    long i;
    def_mdims(NMOS, NP, NRC, NRCE);

    // def_msolver(1, def_DDASAC);
    //def_msolver(1, def_RKF23S);
    def_msolver(1, def_DAESOL);
}

```

```

def_mstage(
    0,
    NXD, NXA, NU,
    NULL, NULL,
    0, 0, 0, NULL, ffcn0, NULL,
    NULL, NULL,
    0
);

for (i=1;i<26;i++){
    def_mstage(
    i,
    NXD, NXA, NU,
    NULL, NULL,
    0, 0, 0, NULL, ffcn1, NULL,
    NULL, NULL,
    0
    );
}

def_lsq(0, "s",0 , 32, lsqfcn1);
for (i=1;i<26;i++){
    def_lsq(i, "s",0 , 2, lsqfcn);
}
}

```

6.3.2 Dat-File

```

* MUSCOD-II/BIOOPT/DAT/LSQ_neu.dat
* (c) Stefan Quint 2005

```

```

* # of multiple shooting intervals on each model stage
nshoot
0: 1
1: 1
2: 1
3: 1

```

4: 1
5: 1
6: 1
7: 1
8: 1
9: 1
10: 1
11: 1
12: 1
13: 1
14: 1
15: 1
16: 1
17: 1
18: 1
19: 1
20: 1
21: 1
22: 1
23: 1
24: 1
25: 1
26: 1

* model stage duration start values, scale factors, and bounds

h

0: 1000000

1: 30

2: 10

3: 10

4: 10

5: 10

6: 10

7: 10

8: 10

9: 10

10: 10

11: 10

12: 10

13: 10
14: 10
15: 10
16: 10
17: 10
18: 10
19: 10
20: 10
21: 20
22: 20
23: 20
24: 20
25: 20
26: 200

plot_first
1

plot_last
26

h_sca
0: 1.0
1: 1.0
2: 1.0
3: 1.0
4: 1.0
5: 1.0
6: 1.0
7: 1.0
8: 1.0
9: 1.0
10: 1.0
11: 1.0
12: 1.0
13: 1.0
14: 1.0
15: 1.0
16: 1.0

17: 1.0
18: 1.0
19: 1.0
20: 1.0
21: 1.0
22: 1.0
23: 1.0
24: 1.0
25: 1.0
26: 1.0

h_min

0: 0
1: 0
2: 0
3: 0
4: 0
5: 0
6: 0
7: 0
8: 0
9: 0
10: 0
11: 0
12: 0
13: 0
14: 0
15: 0
16: 0
17: 0
18: 0
19: 0
20: 0
21: 0
22: 0
23: 0
24: 0
25: 0
26: 0

h_max

0: 200

1: 200

2: 200

3: 200

4: 200

5: 200

6: 200

7: 200

8: 200

9: 200

10: 200

11: 200

12: 200

13: 200

14: 200

15: 200

16: 200

17: 200

18: 200

19: 200

20: 200

21: 200

22: 200

23: 200

24: 200

25: 200

26: 200

h_fix

0: 1

1: 1

2: 1

3: 1

4: 1

5: 1

6: 1

7: 1

8: 1

9: 1
10: 1
11: 1
12: 1
13: 1
14: 1
15: 1
16: 1
17: 1
18: 1
19: 1
20: 1
21: 1
22: 1
23: 1
24: 1
25: 1
26: 1

h_name

0: !
1: !
2: !
3: !
4: !
5: !
6: !
7: !
8: !
9: !
10: !
11: !
12: !
13: !
14: !
15: !
16: !
17: !
18: !
19: !

20: !
21: !
22: !
23: !
24: !
25: !
26: !

* specification mode for differential state variable start values
s_spec
2

* differential state start values, scale factors, and bounds

sd(0,0)
0: 0
1: 5.9979
2: 1.6107e-4
3: 0.0591337
4: 8.52489e-4
5: 0.00358227
6: 2.75154e-4
7: 1.42516e-4
8: 0.00366873
9: 0.202676
10: 0.0010836
11: 6.08921e-6
12: 1.06712e-5
13: 7.3411e-6

sd_fix(0,0)
0: 1
1: 1
2: 1
3: 1
4: 1
5: 1
6: 1
7: 1
8: 1

9: 1
10: 1
11: 1
12: 1
13: 1

sd_sca(*,*)

0: 1
1: 1
2: 1
3: 1
4: 1
5: 1
6: 1
7: 1
8: 1
9: 1
10: 1
11: 1
12: 1
13: 1

sd_min(*,*)

0: -100000
1: -100000
2: -100000
3: -100000
4: -100000
5: -100000
6: -100000
7: -100000
8: -100000
9: -100000
10: -100000
11: -100000
12: -100000
13: -100000

sd_max(*,*)

0: 100000

1: 100000
2: 100000
3: 100000
4: 100000
5: 100000
6: 100000
7: 100000
8: 100000
9: 100000
10: 100000
11: 100000
12: 100000
13: 100000

xd_name

0: x1
1: x2
2: x3
3: x4
4: x5
5: x6
6: x7
7: x8
8: x9
9: x10
10: x11
11: x12
12: x13
13: x14

P

0: 0.312
1: 0.296
2: 0.05
3: 0.83
4: 0.017
5: 0.06705
6: 0.09
7: 0.79
8: 0.188

9: 0.05
10: 0.3
11: 0.0225
12: 0.05
13: 0.014
14:0.69
15:0.11
16:0.043
17:0.0001
18: 0.014
19:0.0177
20:0.00208
21:0.00301
22:4.39314
23:0.0101
24:0.0001
25:0.00002
26:3.1
27:0.23
28:0.045
29:0.5
30: 1
31: 0.01

p_fix

0: 0
1: 0
2: 0
3: 0
4: 0
5: 0
6: 0
7: 0
8: 0
9: 0
10: 0
11: 0
12: 0
13: 0
14: 0

15: 0
16: 0
17: 0
18: 0
19: 0
20: 0
21: 0
22: 0
23: 0
24: 0
25: 0
26: 0
27: 0
28: 0
29: 0
30: 0
31: 1

p_sca

0: 1
1: 1
2: 1
3: 1
4: 1
5: 1
6: 1
7: 1
8: 1
9: 1
10: 1
11: 1
12: 1
13: 1
14: 1
15: 1
16: 1
17: 1
18: 1
19: 1
20: 1

21: 1
22: 1
23: 1
24: 1
25: 1
26: 1
27: 1
28: 1
29: 1
30: 1
31: 1

p_min

0: 0
1: 0
2: 0
3: 0
4: 0
5: 0
6: 0
7: 0
8: 0
9: 0
10: 0
11: 0
12: 0
13: 0
14: 0
15: 0
16: 0
17: 0
18: 0
19: 0
20: 0
21: 0
22: 0
23: 0
24: 0
25: 0
26: 0

27: 0
28: 0
29: 0
30: 0
31: 0

p_max

0: 200
1: 200
2: 200
3: 200
4: 200
5: 200
6: 200
7: 200
8: 200
9: 200
10: 200
11: 200
12: 200
13: 200
14: 200
15: 200
16: 200
17: 200
18: 200
19: 200
20: 200
21: 200
22: 200
23: 200
24: 200
25: 200
26: 200
27: 200
28: 200
29: 200
30: 200
31: 200

p_name
0: !k1
1: !k2
2: !k3
3: !k4
4: !k5
5: !k6
6: !k7
7: !k8
8: !k9
9: !k10
10: !k11
11: !k12
12: !k13
13: !k14
14: !k15
15: !k16
16: !k17
17: !k18
18: !k19
19: !k20
20: !k21
21: !k22
22: !k23
23: !k24
24: !k25
25: !k26
26: !c5a
27: !c6a
28: !V
29: !KM
30: !Vi
31: !KMi

of_sca
1000

of_min
0

of_max

5

of_name

least squares

nhist

20